Phase behavior and topological defects of self-propelled particles in 2D

Pasquale Digregorio
PhD student - Università degli Studi di Bari “Aldo Moro”, INFN - Sezione di Bari
pasquale.digregorio@ba.infn.it

PhD thesis defense - 17 March 2020

Outline

The main motivation of this work is to analyze the aggregation phenomena of bidimensional out-of-equilibrium self-propelled particles on the ground of the standard Kosterlitz-Thouless 2D phase transition theory.

Outline

The main motivation of this work is to analyze the aggregation phenomena of bidimensional out-of-equilibrium self-propelled particles on the ground of the standard Kosterlitz-Thouless 2D phase transition theory.

- Introduction to self-propelled particle systems;
- overview of KTHN theory of melting for 2D particle systems;
- main results and phase diagram of self-propelled disks;
- isolated and extended topological defects;
- self-propelled elongated particles: dumbbells.

Self-propelled disks

Self-propelled particles are able to sustain their own motion, extracting energy from the environment. For this reason they are named “active”. Self-propulsion breaks detailed balance and drives the system out of thermal equilibrium.

Standard random walk

Persistent random walk

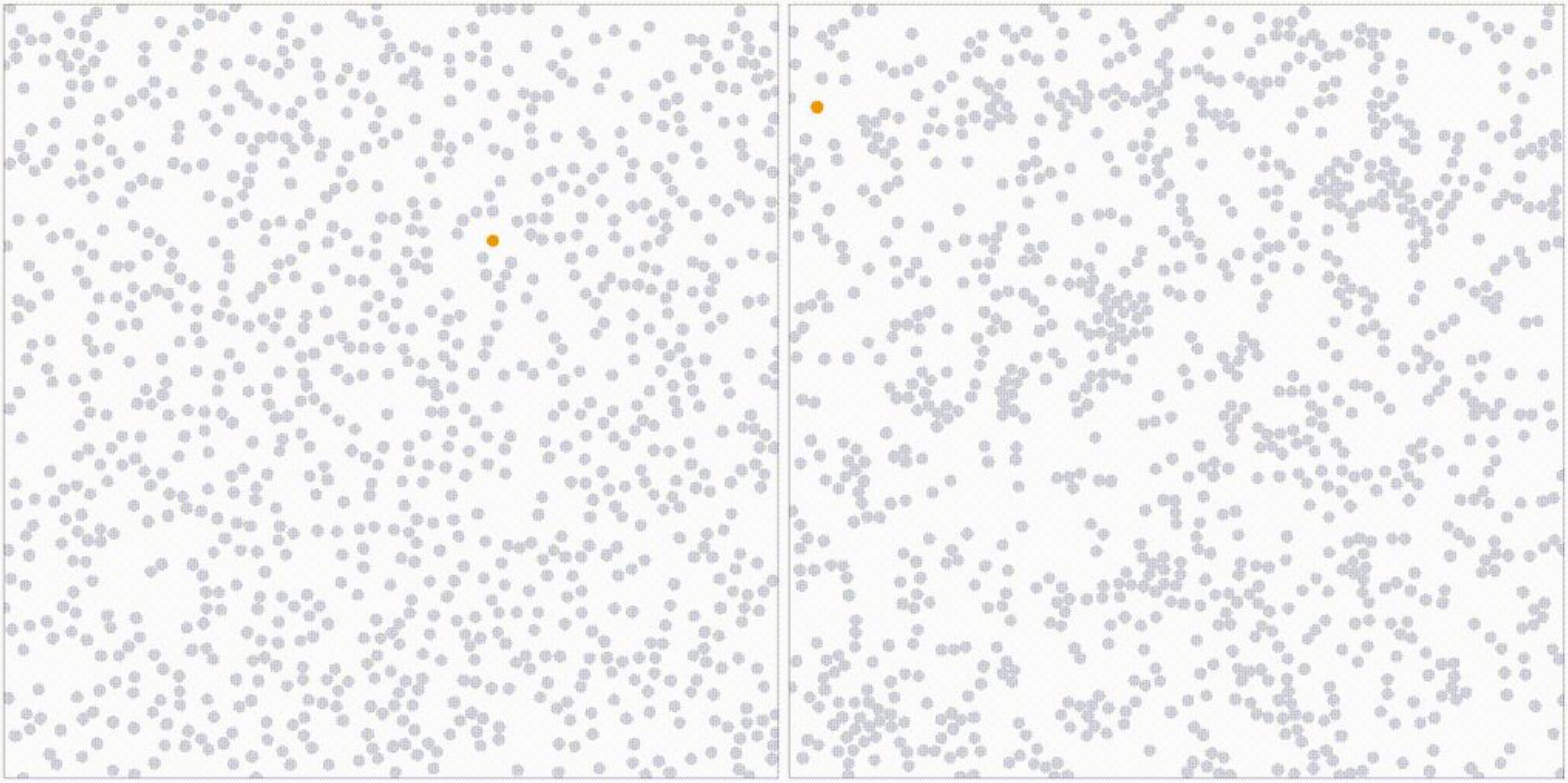

Self-propelled (active) brownian disks

$$\mathbf{n}_i = (\cos\theta_i(t), \sin\theta_i(t))$$
$$\gamma\dot{\mathbf{r}}_i = F_{act}\mathbf{n}_i - \nabla_i \sum_{j(\neq i)} U(r_{ij}) + \sqrt{2\gamma k_B T}\,\xi_i, \qquad \dot{\theta}_i = \sqrt{2D_\theta}\,\eta_i$$

- $U(r) = \begin{cases} U_{\text{Mie}}(r) - U_{\text{Mie}}(r_{min}) & \text{if } r < r_{min} \\ 0 \quad \text{if } r \geqslant r_{min} \end{cases}$
- $\langle \xi_i^\alpha(t) \rangle = 0, \quad \langle \xi_i^\alpha(t)\ \xi_j^\beta(t') \rangle = \delta_{ij}\delta^{\alpha\beta}\delta(t-t')$
- $\langle \eta_i(t) \rangle = 0, \quad \langle \eta_i(t)\ \eta_j(t') \rangle = \delta_{ij}\delta(t-t')$
- $D_\theta = 3k_BT/\gamma\sigma_d^2$

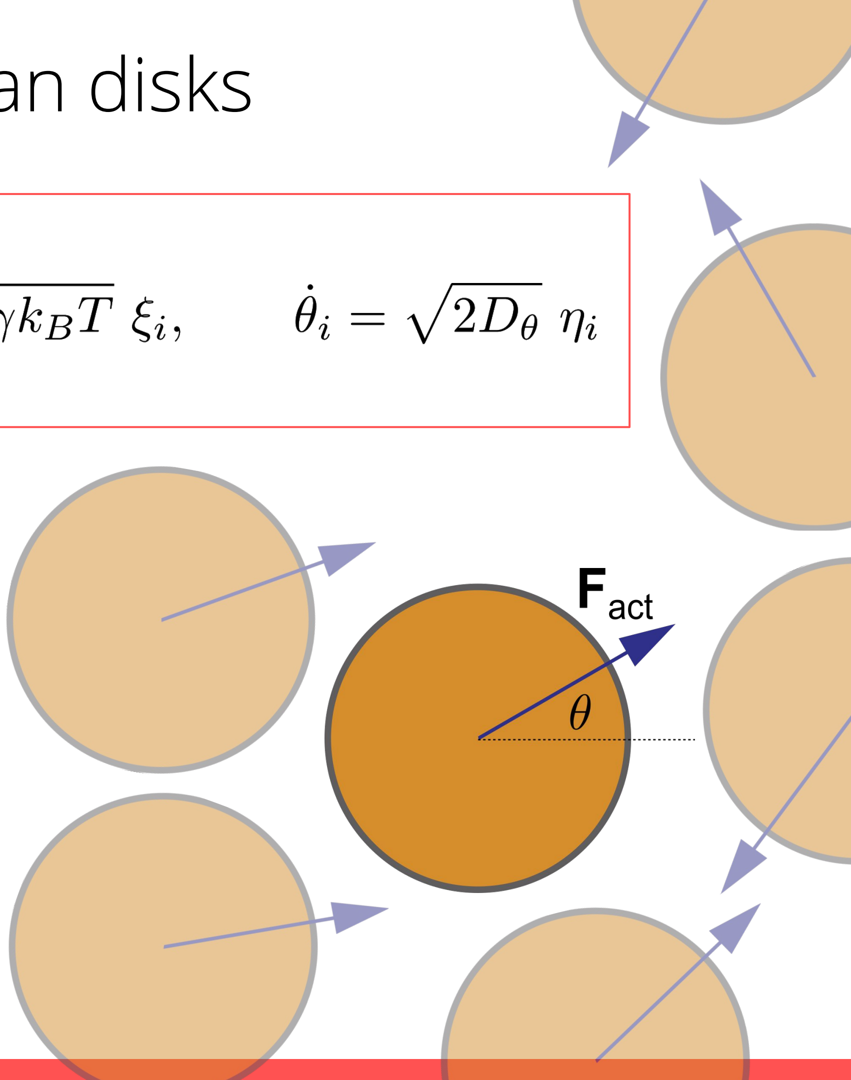

Self-propelled (active) brownian disks

$$\mathbf{n}_i = (\cos\theta_i(t), \sin\theta_i(t))$$

$$\gamma\dot{\mathbf{r}}_i = F_{act}\mathbf{n}_i - \nabla_i \sum_{j(\neq i)} U(r_{ij}) + \sqrt{2\gamma k_B T}\,\xi_i, \qquad \dot{\theta}_i = \sqrt{2D_\theta}\,\eta_i$$

- Surface fraction: $\phi = N\dfrac{\pi\sigma_d^2}{4S}$
- Péclet number: $\mathrm{Pe} = \dfrac{Lv_{act}}{D} = \dfrac{\sigma_d F_{act}}{k_B T}$

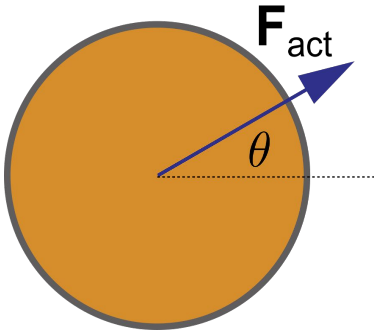

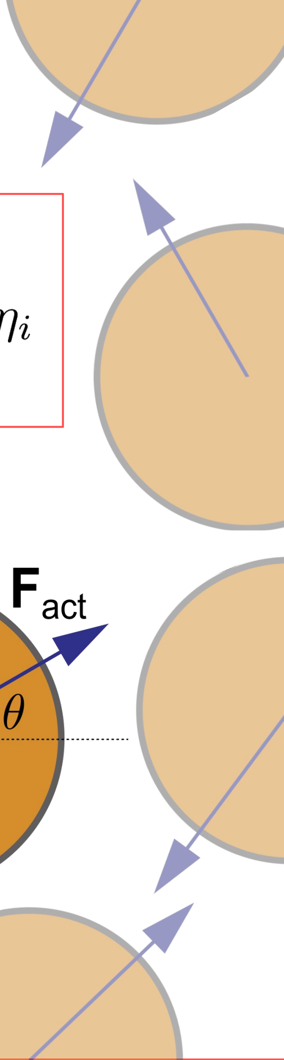

Persistent random walk

Equations of motion for dilute system

$$\mathbf{n}(t) = \big(\cos\theta(t), \sin\theta(t)\big)$$

$$\boxed{\gamma\dot{\mathbf{r}}(t) = F_{\mathrm{act}}\ \mathbf{n}(t) + \sqrt{2\gamma k_B T}\ \xi(t), \qquad \dot{\theta}(t) = \sqrt{2D_\theta}\ \eta(t)}$$

The polarization is correlated over a *persistence time* $\tau_{\mathrm{p}} = 1/D_\theta$

$$\langle \mathbf{n}(t)\cdot\mathbf{n}(t_0)\rangle = \mathrm{e}^{-D_\theta(t-t_0)}$$

$$\langle (\mathbf{r}(t)-\mathbf{r}(t_0))^2\rangle = \frac{4k_BT}{\gamma}(t-t_0) + 2\left(\frac{F_{\mathrm{act}}}{\gamma}\right)^2 \frac{1}{D_\theta^2}\left[D_\theta(t-t_0) + \mathrm{e}^{-D_\theta(t-t_0)} - 1\right]$$

At short times $(t-t_0) \ll \tau_{\mathrm{p}}$ ballistic motion emerges with *persistence velocity* $v_0 = F_{\mathrm{act}}/\gamma$.

Diffusive regime at long times with enhanced diffusion coefficient $D_{\mathrm{eff}} = D_0 + \dfrac{v_0^2}{2D_\theta}$.

Self-propelled particle systems and persistent random walk are able to captures the key feature of living agents.

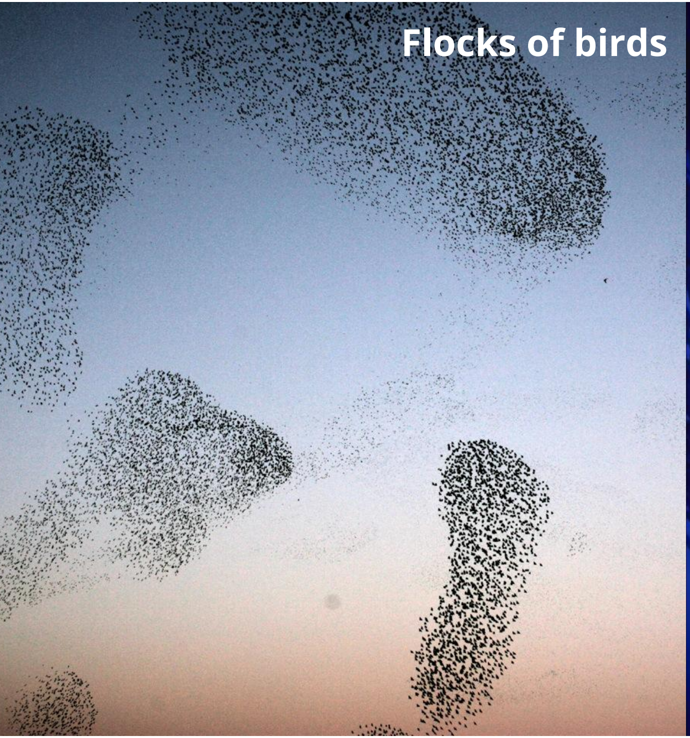

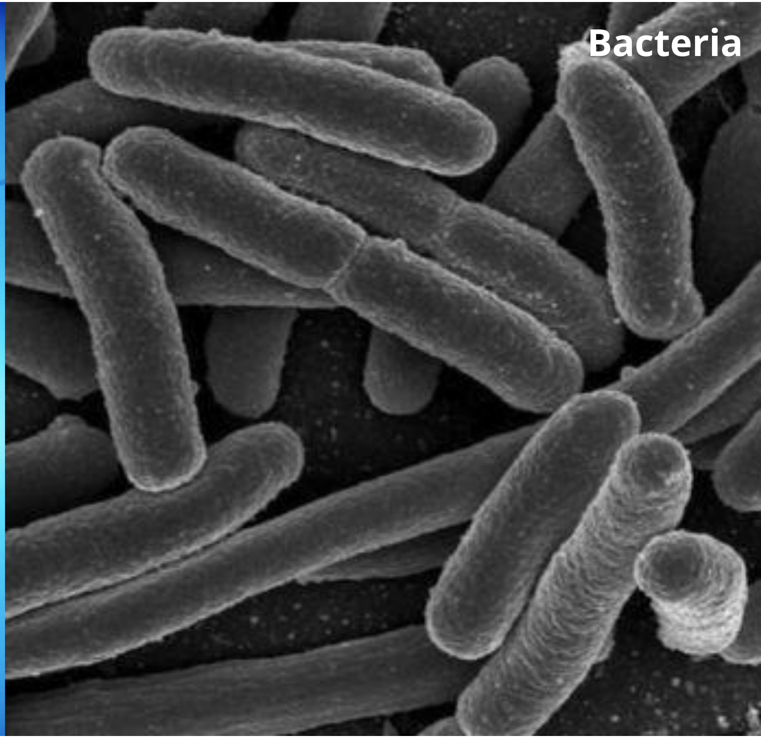

Vicsek T., Czirók A., Ben-Jacob E., Cohen I., Shochet. O., Phys. Rev. Lett., 75:1226–1229, (1995)
Wu X., Libchaber A., Phys. Rev. Lett., 84:3017, (2000)

Experimental realizations exist, which allow to study the properties of active matter, with the aim to exploit them for technological uses, like for instance micro-motors, or delivery at the microscale.

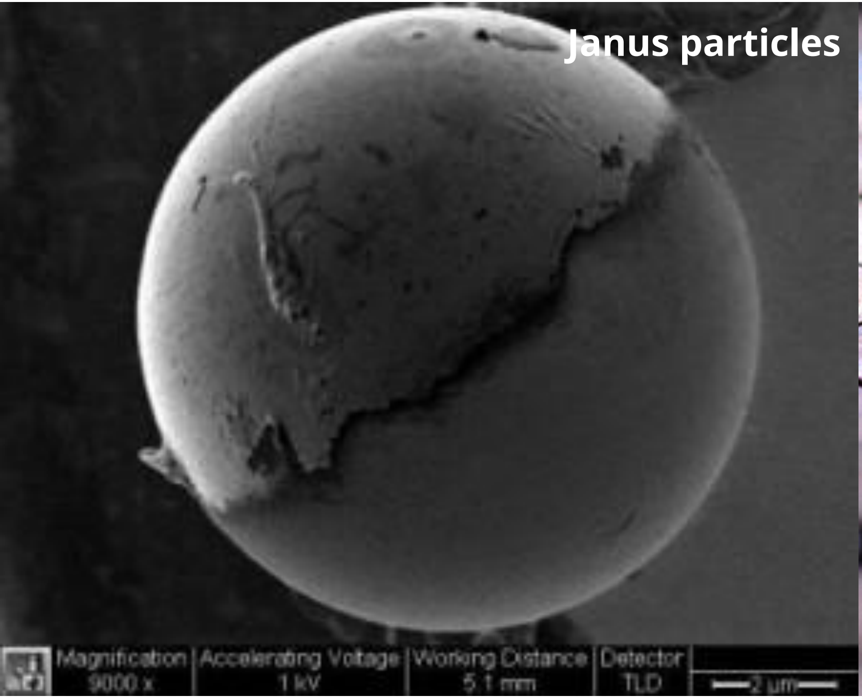

Buttinoni I., *et al.,* Phys.Rev.Lett., 110 238301, (2013)
Ginot F., et al., Phys. Rev. X, 5 011004, (2015)

Dauchot O., *et al.* Phys. Rev. Lett., 105 098001, (2010)

Motility-induced phase separation (MIPS)

- Self-propelled particles accumulate where they move more slowly.
- They may also slow down at high density.
- Positive feedback can lead to motility-induced phase separation (MIPS) between dense (ordered) and dilute (fluid/gas) phases

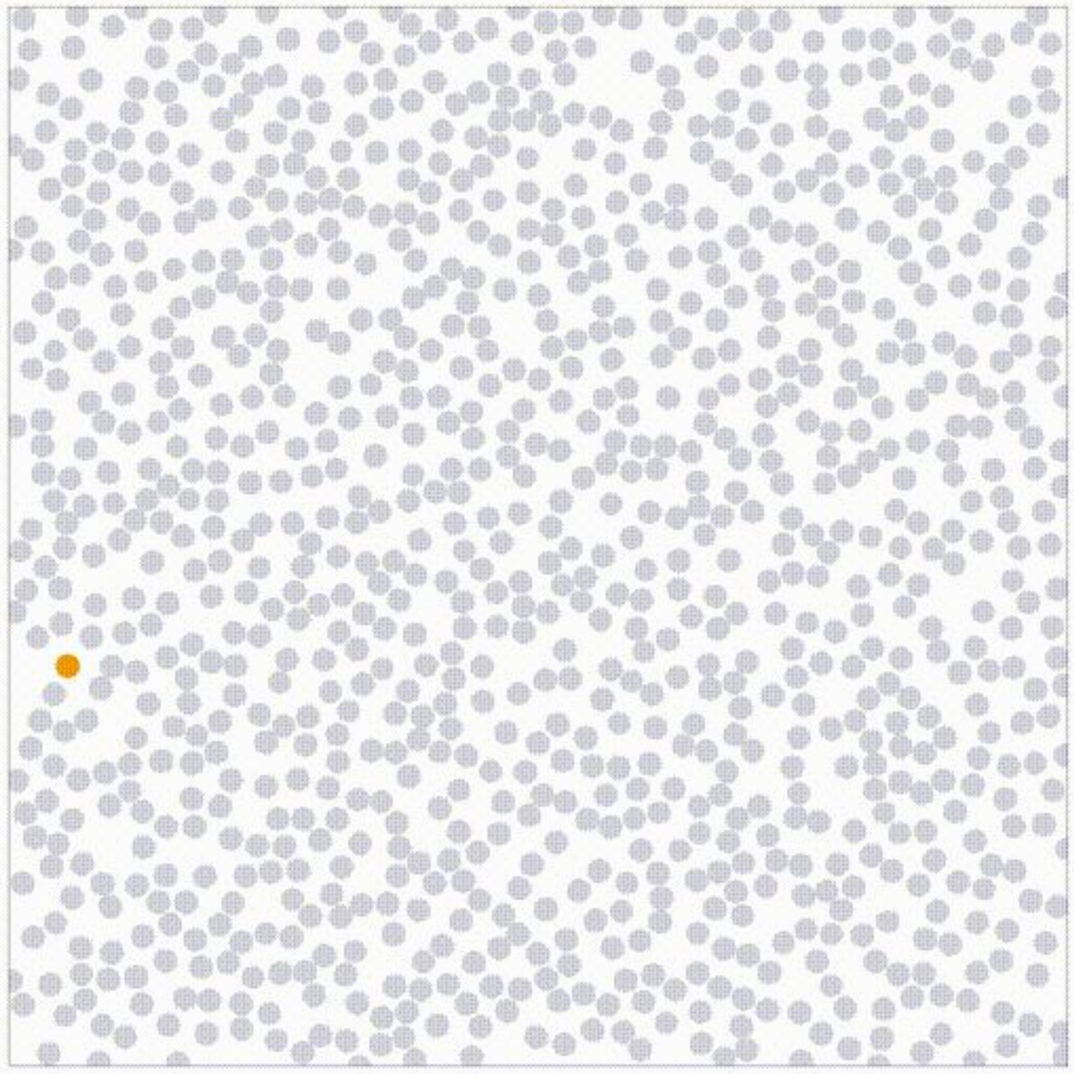

Since motility-induced phase separation (MIPS) involves ordered phases, we aim to address which kind of order is selected by the out-of-equilibrium system (unknown so far).
Later: microscopic mechanism for melting.
The reference theory for equilibrium 2D ordering for particles is the Kosterlitz-Thouless-Halperin-Nelson theory.

Melting of disks in 2D

According to the Kosterlitz-Thouless-Halperin-Nelson theory, melting of short-range interacting disks is a two-step transition from solid to isotropic liquid with intermediate *hexatic* phase.
Both transitions are mediated by unbinding of topological defects.

Phase transitions in 2D: Kosterlitz-Thouless-Halperin-Nelson

LIQUID ? **SOLID** ϕ

Translational order

short-ranged

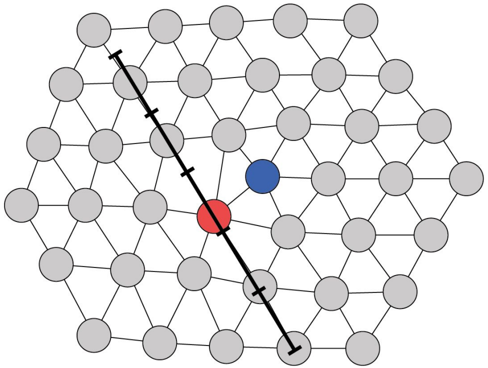

quasi-long-ranged

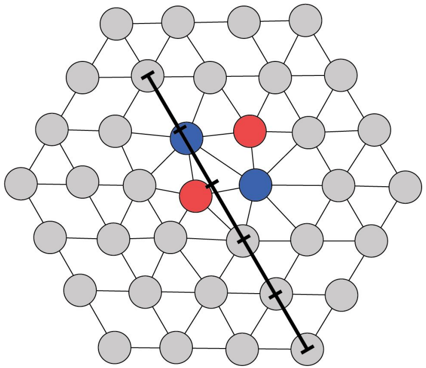

The Mermin-Wagner theorem states that true long-ranged order does not exist in $D < 3$, because thermal fluctuations diverge with the system size.
Only *quasi-long-ranged* order exists, which means power-law decaying spatial correlation functions.

Phase transitions in 2D: Kosterlitz-Thouless-Halperin-Nelson

	LIQUID ?	SOLID $\rightarrow \phi$
Translational order	short-ranged	quasi-long-ranged

Red particles have 5 neighbors.
Blue particles have 7 neighbors.

Spatial periodicity in the solid is lost through unbinding of dislocation pairs into free dislocations (5-7 pair).

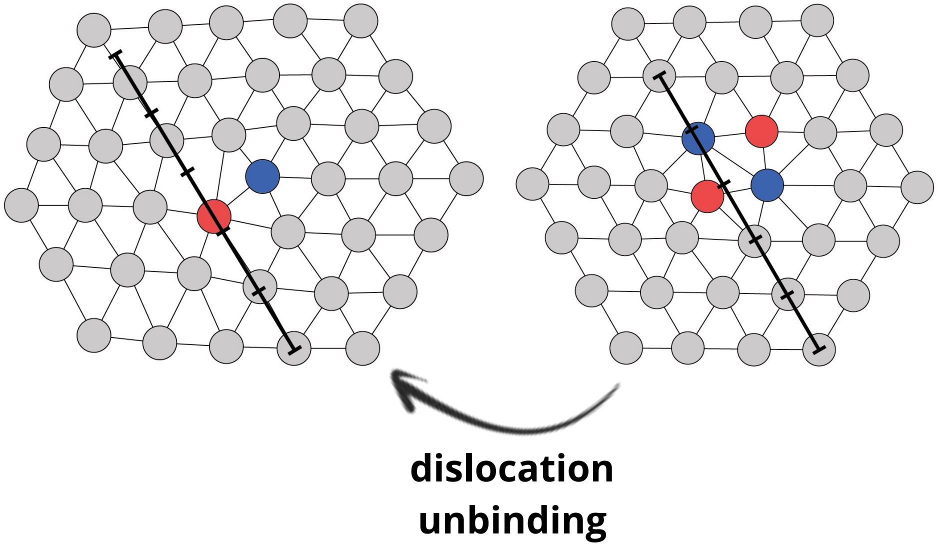

Phase transitions in 2D: Kosterlitz-Thouless-Halperin-Nelson

LIQUID ? **SOLID** ϕ

Translational order short-ranged quasi-long-ranged

Free dislocations allow to preserve bond-orientational periodicity.
New intermediate *hexatic* phase!

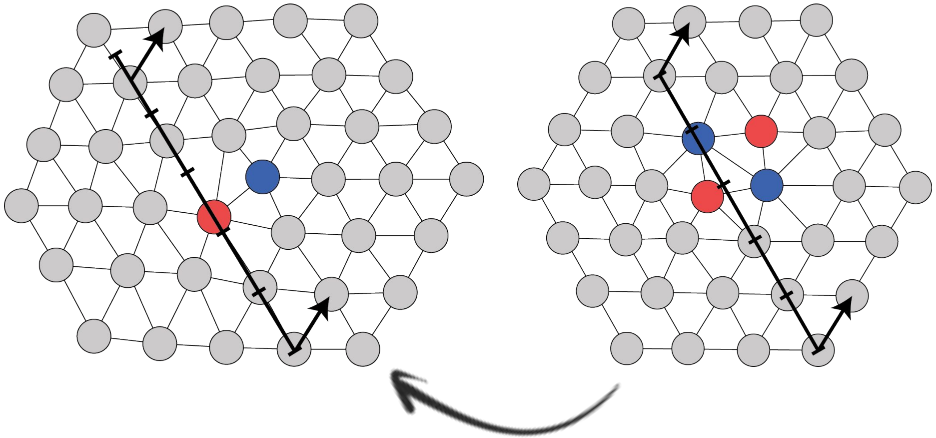

dislocation unbinding

Phase transitions in 2D: Kosterlitz-Thouless-Halperin-Nelson

	LIQUID	HEXATIC	SOLID
Bond-orientational order	short-ranged	quasi-long-ranged	long-ranged
Translational order	short-ranged	short-ranged	quasi-long-ranged

ϕ

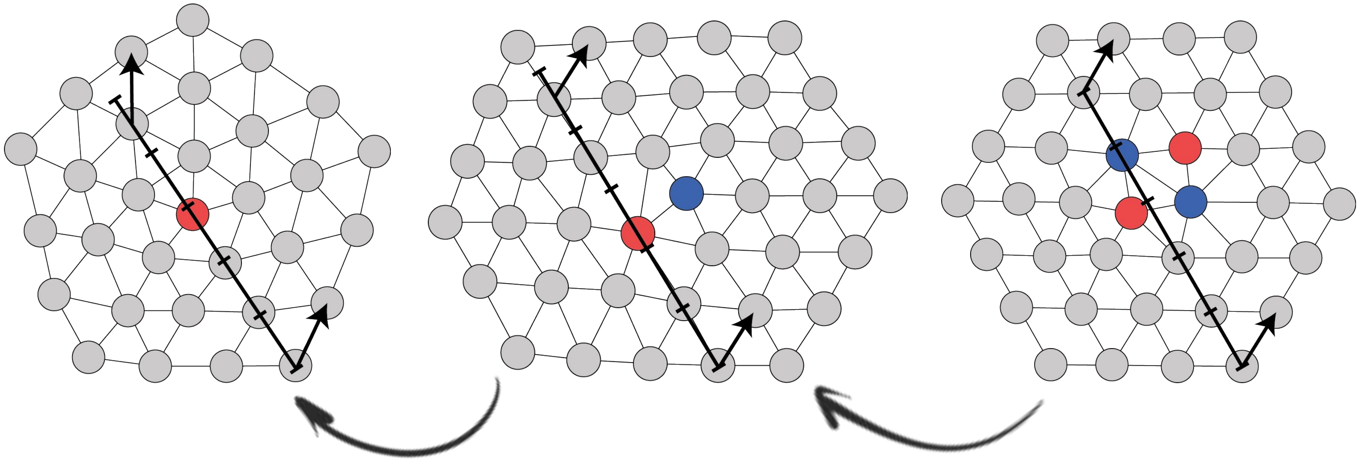

disclination unbinding

dislocation unbinding

Phase transitions in 2D: Kosterlitz-Thouless-Halperin-Nelson

	LIQUID	**HEXATIC**	**SOLID**
Bond-orientational order	short-ranged	quasi-long-ranged	long-ranged
Translational order	short-ranged	short-ranged	quasi-long-ranged

ϕ

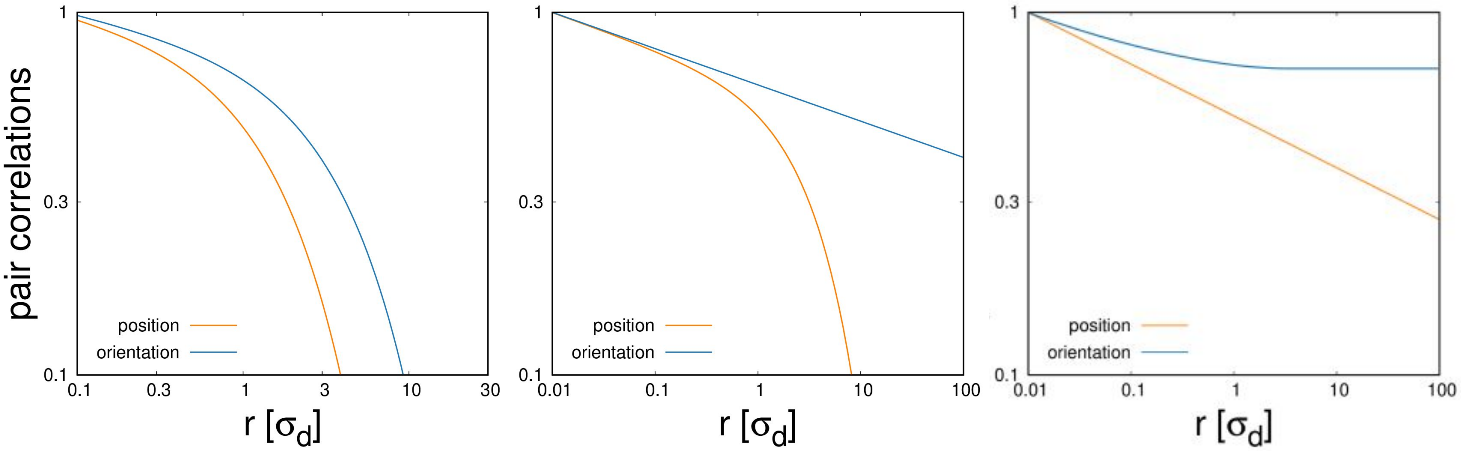

Melting scenario for hard disks. Recent results

- First order phase transition between liquid and hexatic
- KTHN transition between hexatic and solid

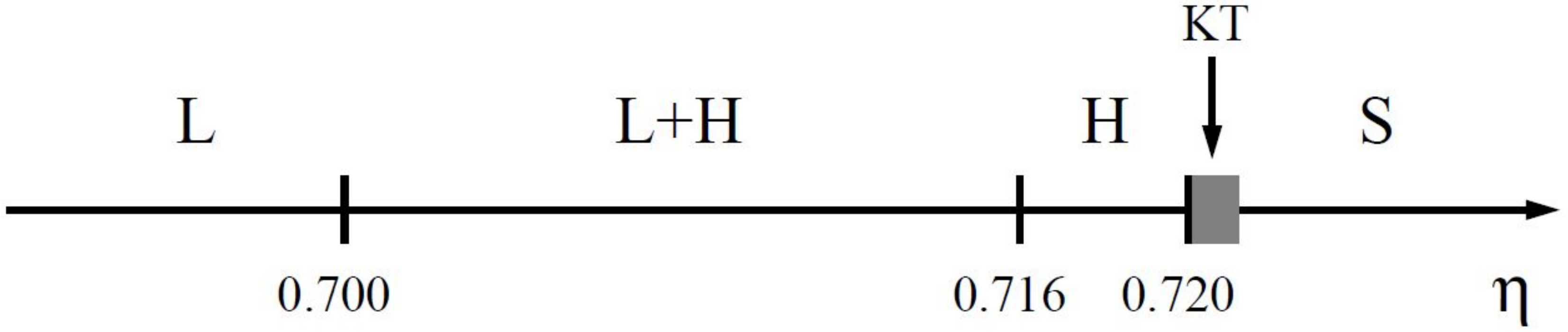

Bernard P., Krauth W. F., Phys. Rev. Lett., 107 155704, (2015)
Dullens P.A., *et al.*, Phys. Rev. Lett., 118 158001 (2017)
Cugliandolo L.F., DP, Gonnella G., Suma A., Phys. Rev. Lett. 119, 268002, (2017)

Phase diagram of active disks

By means of large-scale MD simulations, we explored translational and orientational order for a system of SP hard disks for global packing fraction in the range $[0:\phi_{\rm cp}]$ and Péclet number in the range $[0:200]$ (self-propulsion velocity in $[0:1]$, units of particle diameter and interaction energy).

Phase diagram for active disks

Solid

Hexatic

Coexistence

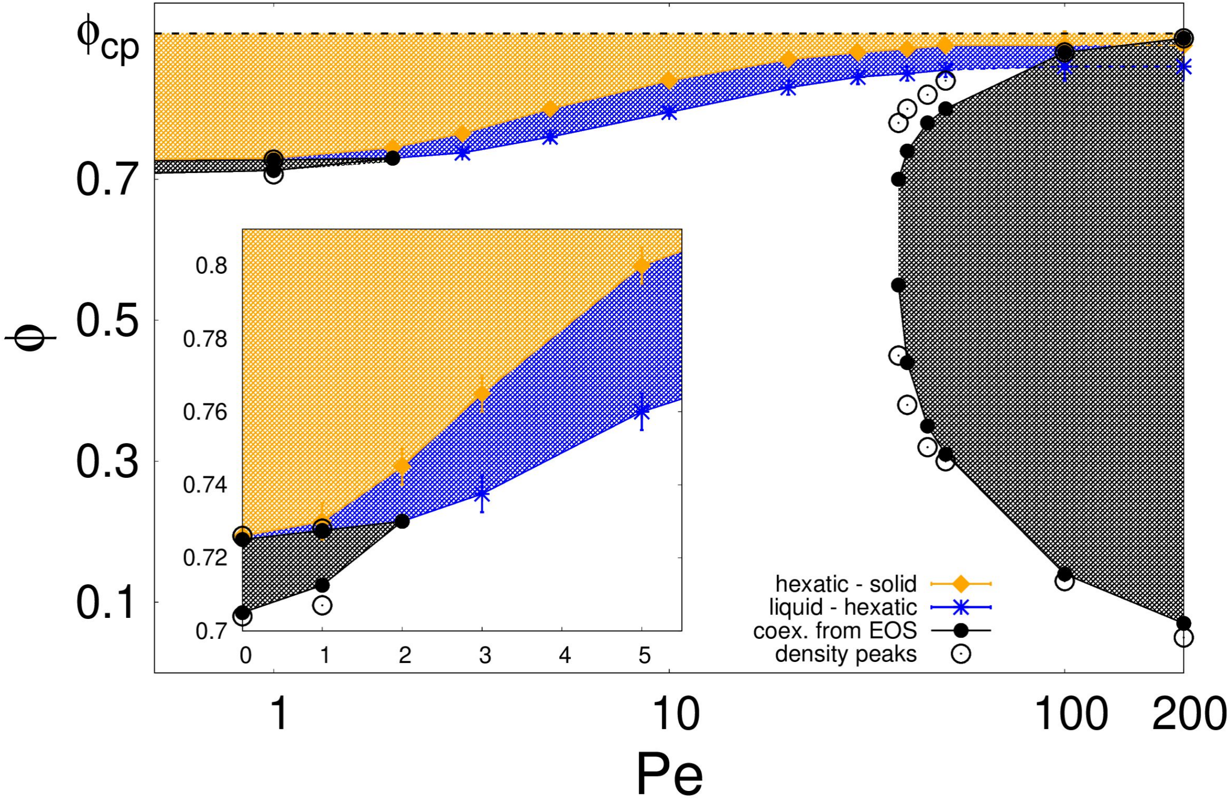

DP, Levis D., Suma A., Cugliandolo L.F., Gonnella G., Pagonabarraga I., Phys. Rev. Lett., 121 098003 (2018)

Phase diagram for active disks

Spatial correlations of local hexatic parameter allow to recognize quasi-long-ranged bond-orientational order by varying the global surface fraction at fixed Péclet number.

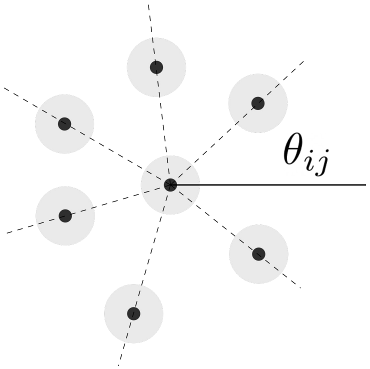

$$\psi_{6i} = \frac{1}{N_i} \sum_{j=1}^{N_i} e^{\mathrm{i}6\theta_{ij}}$$

$$g_6(r) = \frac{\langle \psi_{6i} \psi_{6j}^* \rangle_{r_{ij}=r}}{\langle |\psi_{6i}|^2 \rangle}$$

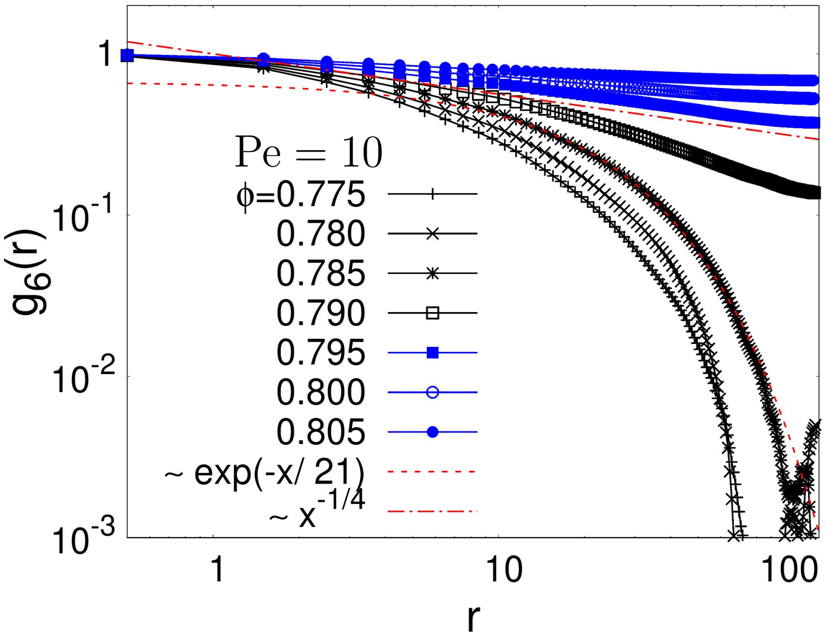

Phase diagram for active disks

Spatial correlations of disks position in the reciprocal space allow to recognize quasi-long-ranged translational order.

$$C_{\mathbf{q}_0}(r) = \langle e^{\mathbf{i}\mathbf{q}_0\cdot(\mathbf{r}_i-\mathbf{r}_j)} \rangle$$

$\mathbf{q}_0$ maximum diffraction peak

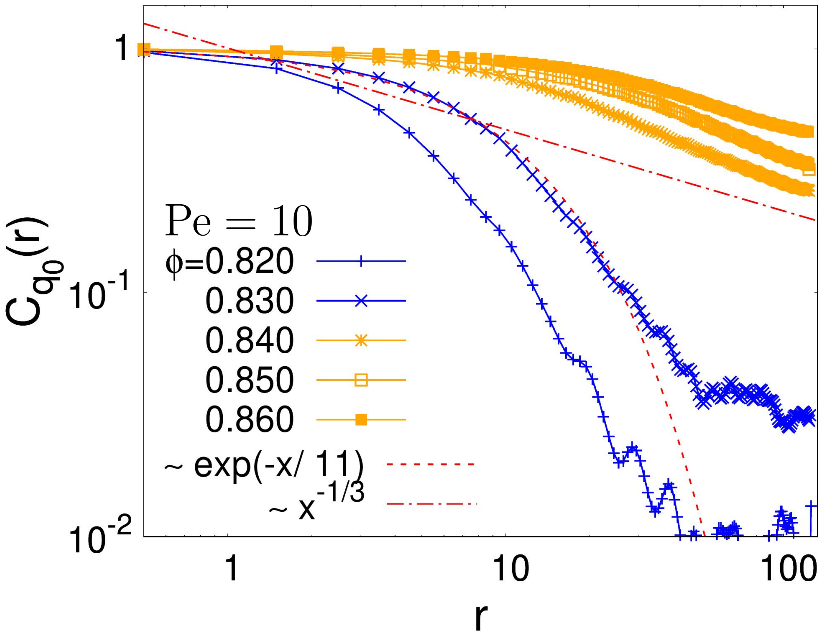

Nature of liquid-hexatic transitions and coexistence

Low-Péclet liq-hex coexistence

Local hexatic

Local density

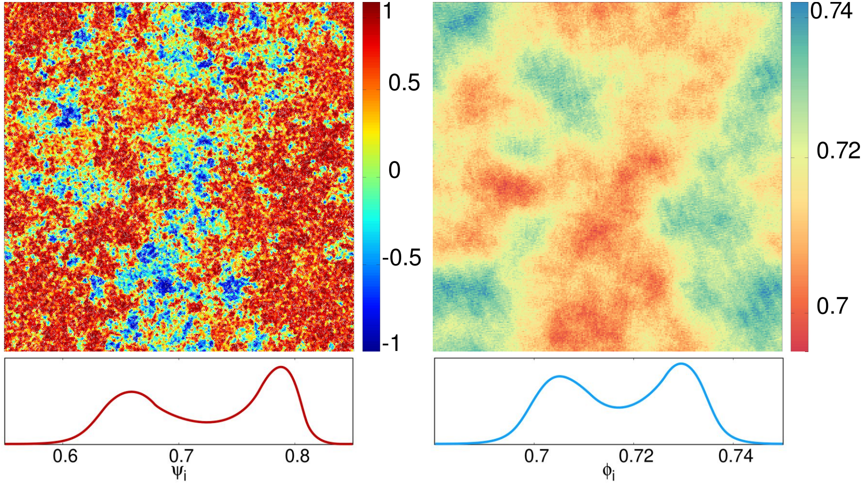

High-Péclet MIPS

Local hexatic

Local density

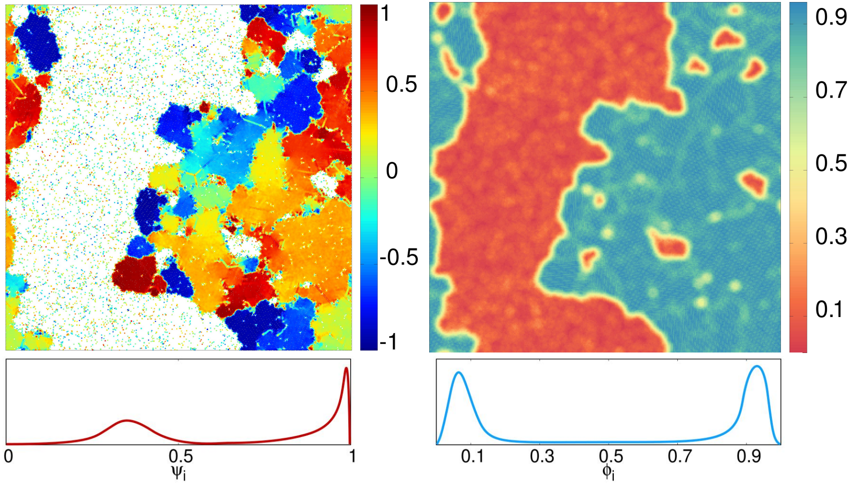

Liquid-hexatic coexistence. Pressure

Having observed coexistence regions from bimodal probability distributions of local parameters, an equation of state can clarify whether this is related to a first-order phase transition.

For self-propelled isotropic particles, a well-defined virial-like equation of state can be constructed. The stress tensor extracted from the microscopic equations of motion satisfies the right conservation laws into the corresponding coarse-grained description.

From the Langevin equations of motion with periodic boundary conditions, separating pair interactions inside the primary box from the ones outside with periodic copies:

Internal pressure | **External pressure**

$$\frac{Nk_BT}{V} + \frac{\gamma v_0}{2V}\sum_i \langle \mathbf{n}_i \cdot \mathbf{r}_i \rangle + \frac{1}{4V}\sum_{ij}\sum_{\mathbf{k}} \langle \mathbf{F}_{ij}^{\mathbf{k}} \cdot (\mathbf{r}_{ij} - \mathbf{R}_{\mathbf{k}}) \rangle = \frac{ND\gamma}{V} - \frac{1}{4V}\sum_{ij}\sum_{\mathbf{k}} \langle \mathbf{F}_{ij}^{\mathbf{k}} \cdot \mathbf{R}_{\mathbf{k}} \rangle$$

With $\mathbf{k}$ running over the periodic images, and D is the diffusion coefficient.

Winkler R.G., Wysocki A., Gompper G.. Soft Matter, 11:6680–6691, 2015.

Liquid-hexatic coexistence. Pressure

$$P = \frac{Nk_BT}{V} + \frac{1}{4V}\sum_{i,j}\sum_{u_x,u_y\in\mathbb{Z}}\langle \mathbf{f}_{ij}\cdot(\mathbf{r}_i-\mathbf{r}_j-\mathbf{R}_\mathbf{u})\rangle + \frac{F_{act}}{2V}\sum_i\langle \mathbf{n}_i\cdot\mathbf{r}_i\rangle$$

Liquid-hexatic coexistence. Pressure

$$P = \boxed{\frac{N k_B T}{V}} + \frac{1}{4V} \sum_{i,j} \sum_{u_x, u_y \in \mathbb{Z}} \langle \mathbf{f}_{ij} \cdot (\mathbf{r}_i - \mathbf{r}_j - \mathbf{R}_\mathbf{u}) \rangle + \frac{F_{act}}{2V} \sum_i \langle \mathbf{n}_i \cdot \mathbf{r}_i \rangle$$

- **Ideal gas**

Liquid-hexatic coexistence. Pressure

$$P = \frac{Nk_BT}{V} + \boxed{\frac{1}{4V}\sum_{i,j}\sum_{u_x,u_y\in\mathbb{Z}}\langle \mathbf{f}_{ij}\cdot(\mathbf{r}_i-\mathbf{r}_j-\mathbf{R_u})\rangle} + \frac{F_{act}}{2V}\sum_i\langle \mathbf{n}_i\cdot\mathbf{r}_i\rangle$$

- Ideal gas
- **internal virial (interactions)**

Liquid-hexatic coexistence. Pressure

$$P = \frac{Nk_BT}{V} + \frac{1}{4V}\sum_{i,j}\sum_{u_x,u_y\in\mathbb{Z}}\langle \mathbf{f}_{ij}\cdot(\mathbf{r}_i - \mathbf{r}_j - \mathbf{R}_\mathbf{u})\rangle + \boxed{\frac{F_{act}}{2V}\sum_i\langle \mathbf{n}_i\cdot\mathbf{r}_i\rangle}$$

- Ideal gas
- internal virial (interactions)
- **active non-conservative virial (swim pressure)**

Liquid-hexatic coexistence. Pressure

$$P = \frac{Nk_BT}{V} + \frac{1}{4V}\sum_{i,j}\sum_{u_x,u_y\in\mathbb{Z}}\langle \mathbf{f}_{ij}\cdot(\mathbf{r}_i - \mathbf{r}_j - \mathbf{R}_\mathbf{u})\rangle + \boxed{\frac{F_{act}}{2V}\sum_i \langle \mathbf{n}_i \cdot \mathbf{r}_i\rangle}$$

- Ideal gas
- internal virial (interactions)
- **active non-conservative virial (swim pressure)**

In the dilute limit:

$$P = \rho k_B T + \frac{\gamma \rho v_0^2}{2D_\theta} = \rho k_B T_{\text{eff}}$$

with T_{eff} effective temperature compatible with the one derived from fluctuation-dissipation relation in the late diffusive regime.

Liquid-hexatic coexistence. Pressure

a) Non monotonic pressure indicates coexistence for both $\mathrm{Pe} = 0$ and low $\mathrm{Pe} > 0$, compatible with pdfs.

c) No coexistence at intermediate activities (KT-type hexatic-liquid).

d) $\mathrm{Pe} = 100$ - MIPS coexistence. Swim pressure drops as the system phase separates, being this term related with the projection of the velocity along the self-propulsion.

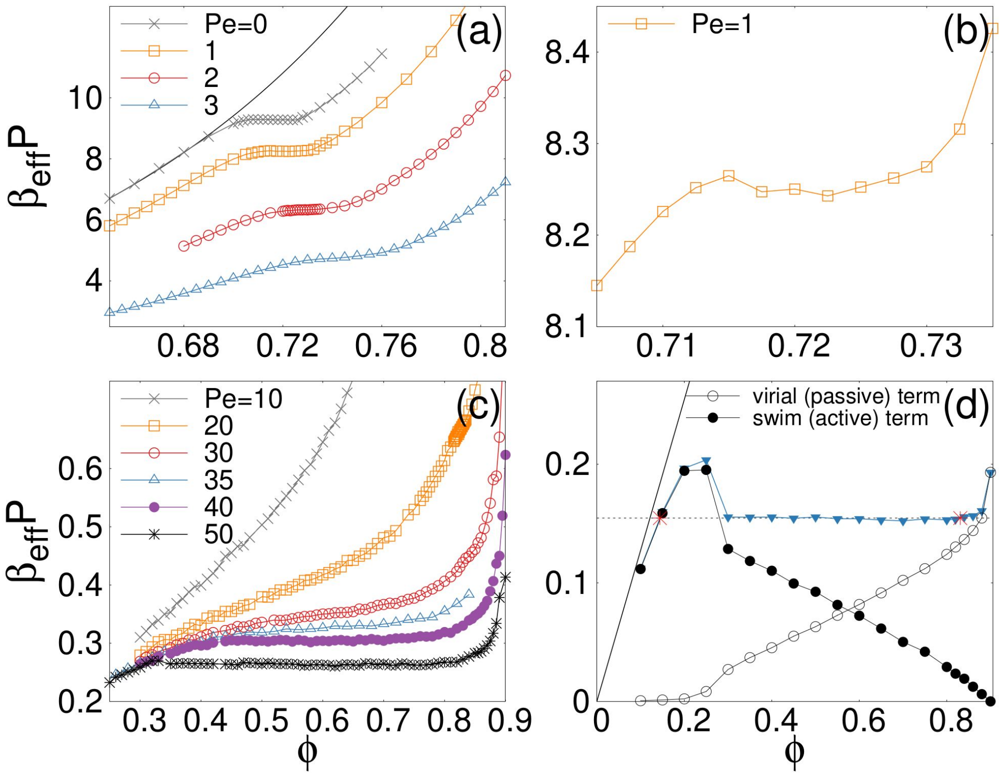

DP, Levis D., Suma A., Cugliandolo L.F., Gonnella G., Pagonabarraga I., Phys. Rev. Lett., 121 098003 (2018)

Topological defects

Having established the phase diagram, we now focus on the microscopic mechanism driving the melting.
Are the solid-hexatic and hexatic-liquid transition for self-propelled disks mediated by unbinding of topological defects, as prescribed by KTHN model for the passive case **?**

We observe an underlying double-step scenario for melting at any activity.
A key role of extended defects emerges in theories of 1st-order melting in 2D, with no strong evidences so far.
1st-order phase transitions are also known to be related to proliferation of extended defects arrays for standard 3D melting (see *e.g.* [Alsayed A.M., *et al.*, Science 309, 1207 (2005)]).

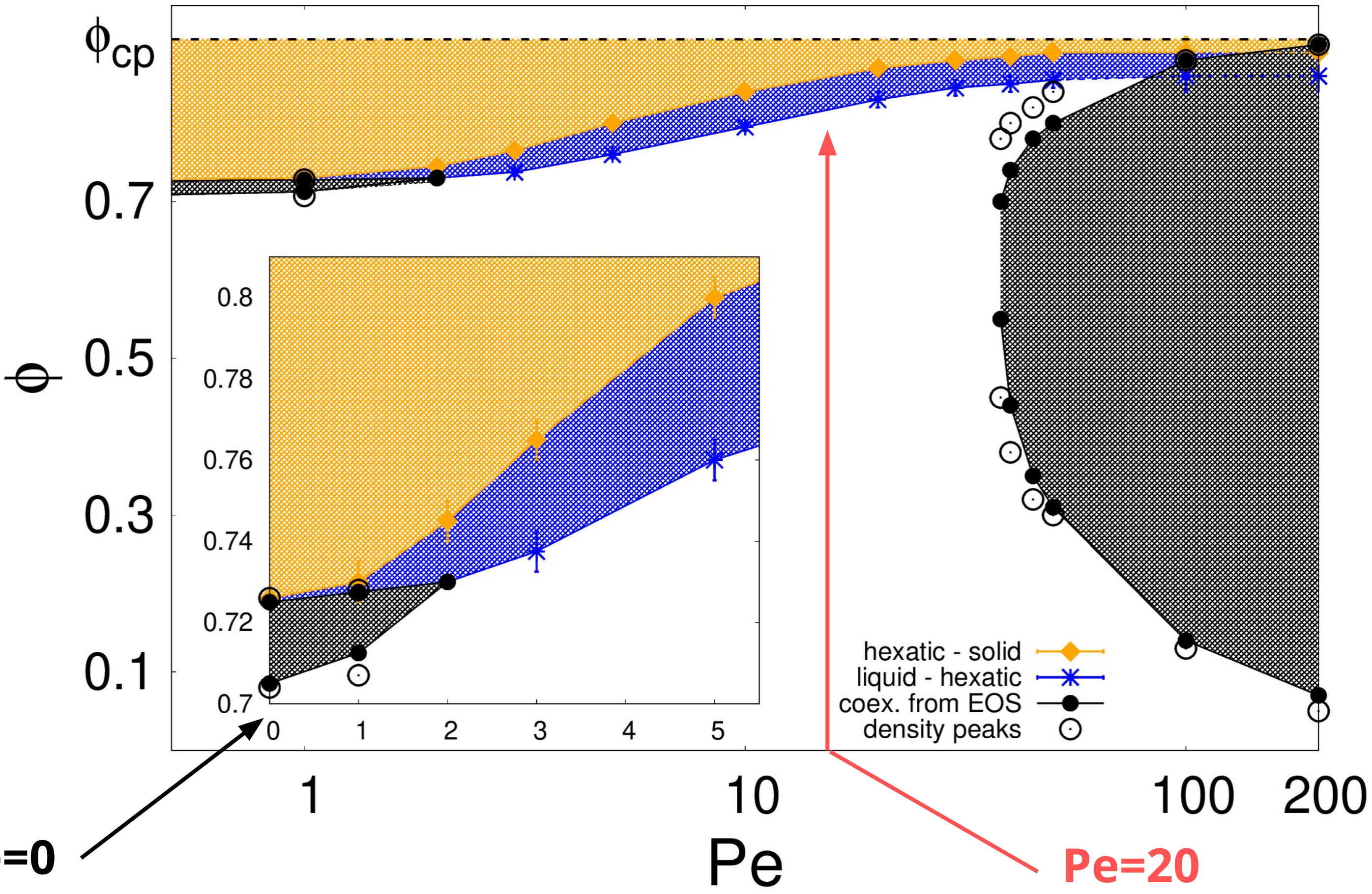

Pe=0
1st-order liq-hex

Pe=20
continuous liq-hex

Halperin-Nelson unbinding mechanism is still present at the transitions in the active system

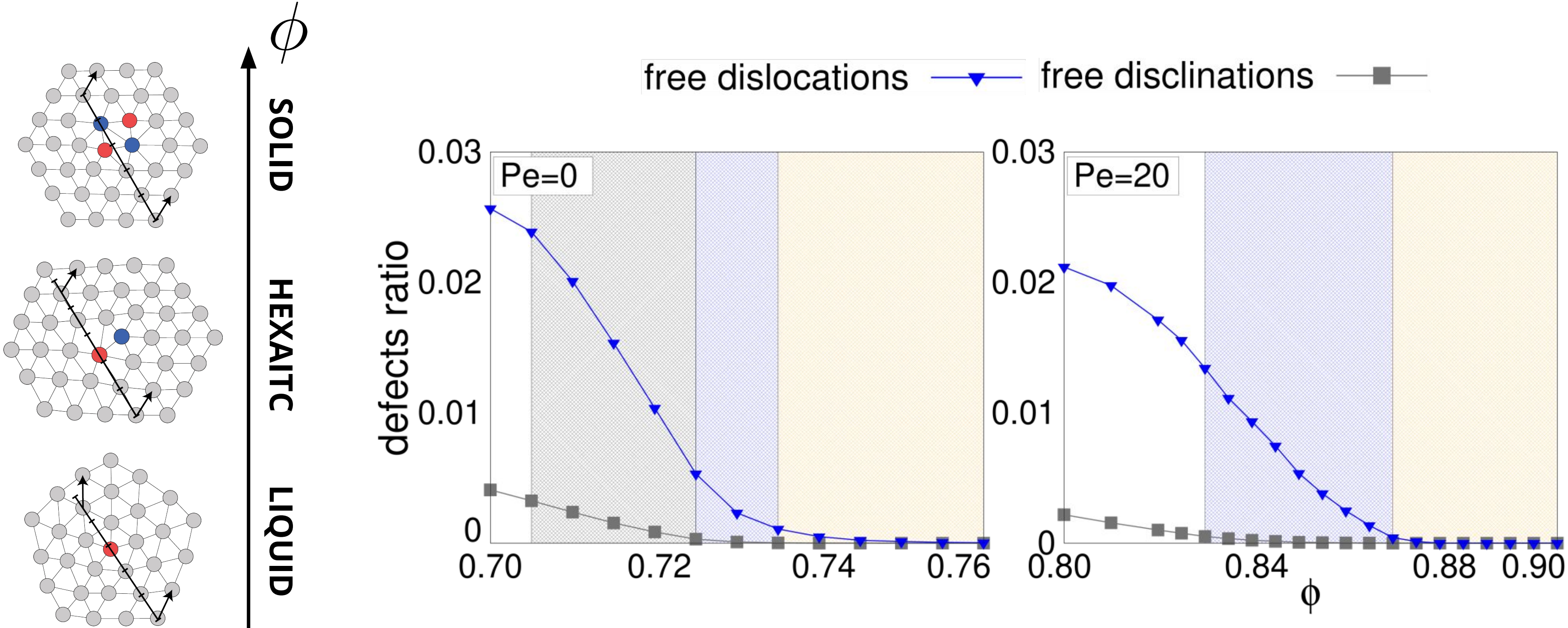

DP, Levis D., Cugliandolo L.F., Gonnella G., Pagonabarraga I., preprint

On top of isolated defects, extended defects clusters are spreadly present

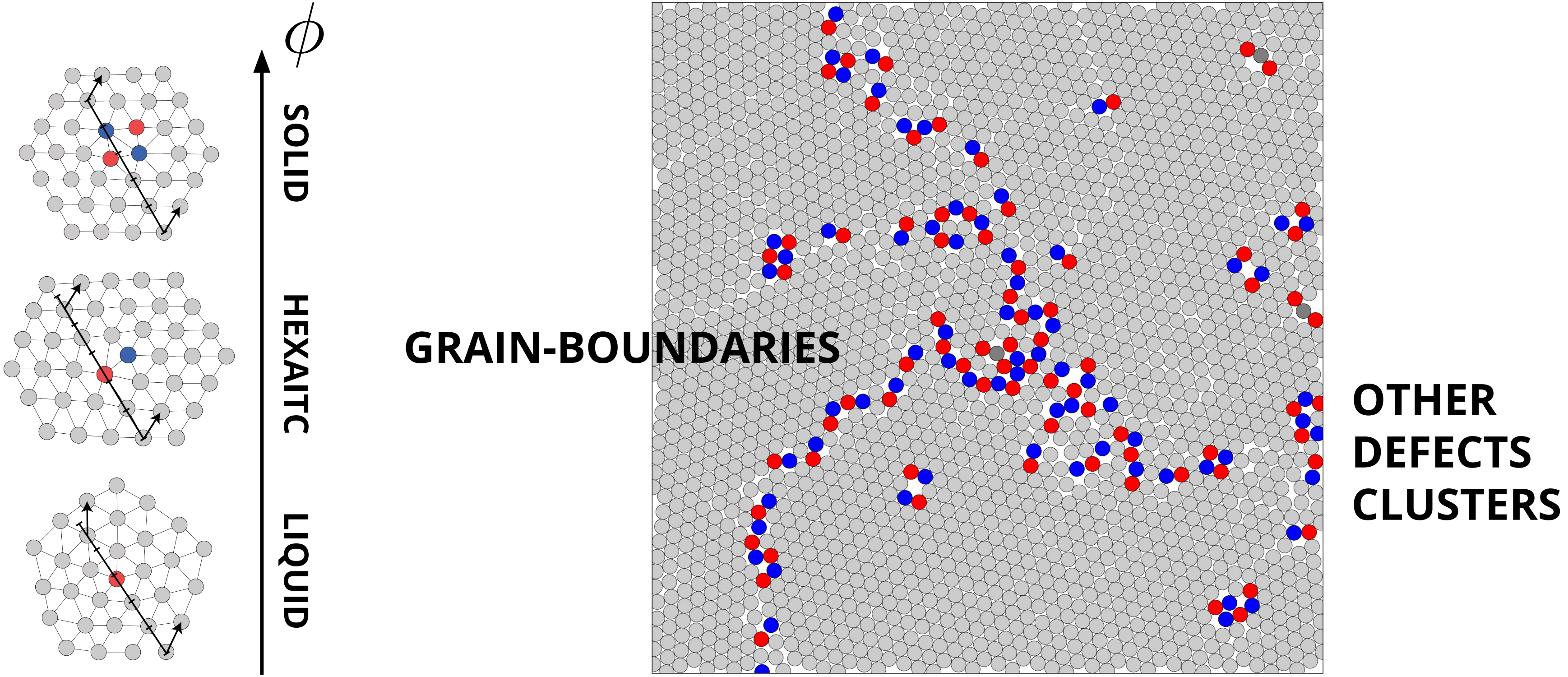

On top of isolated defects, extended defects clusters are spreadly present

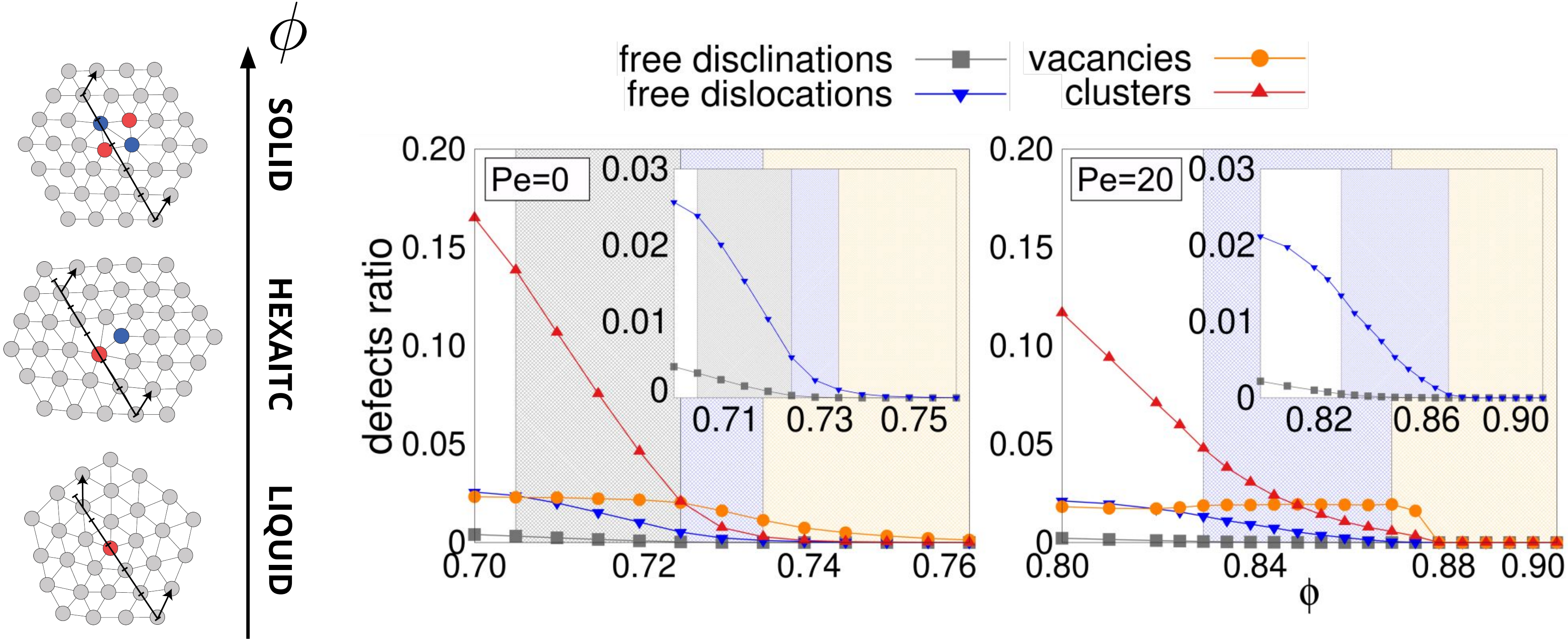

Percolation of defects clusters at the hex-liq melting

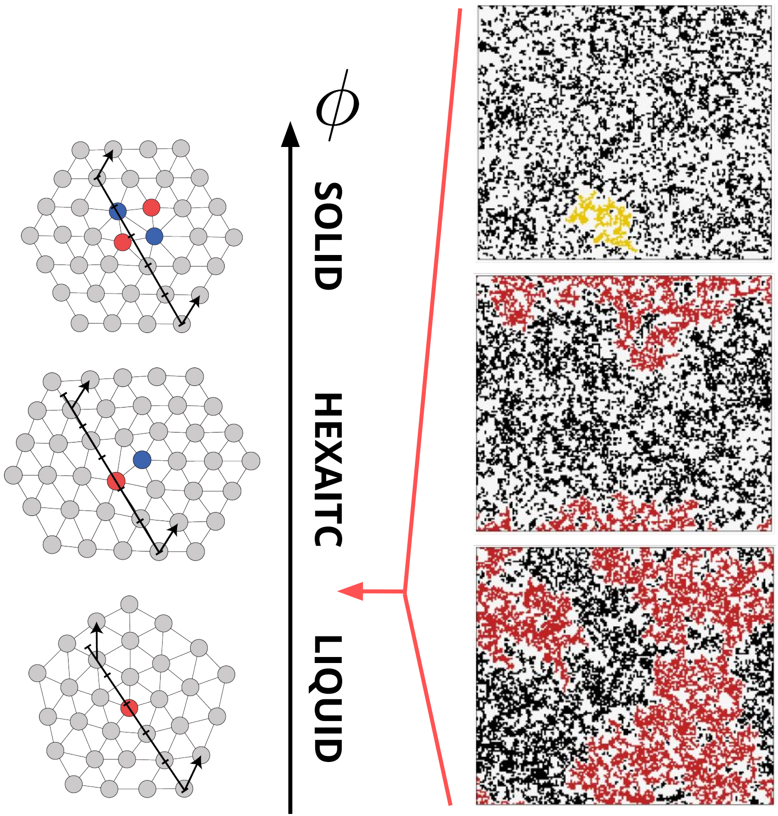

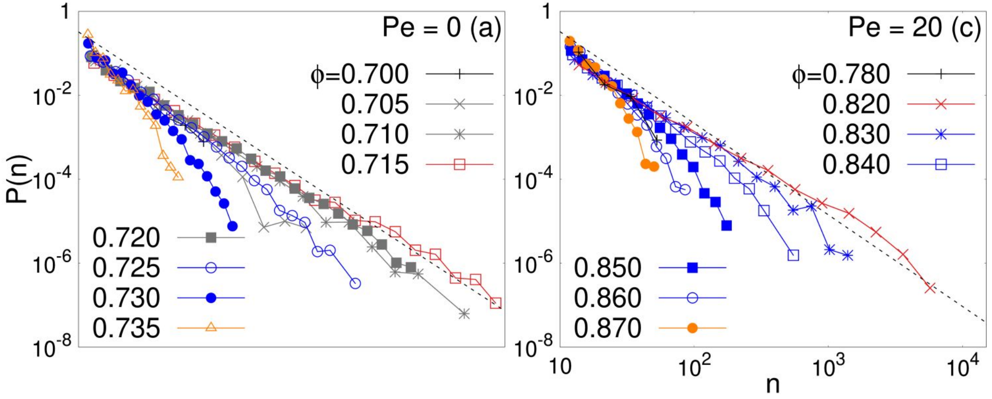

Extended defects percolate in the middle of coexistence or at the hexatic-liquid continuous transition !

Power-law for cluster size distribution at the transition with critical percolation exponent $\tau \simeq 2$.

DP, Levis D., Cugliandolo L.F., Gonnella G., Pagonabarraga I., preprint

Similarly to 3D melting, the liquid starts to form along the grain-boundaries between the hexatic domains

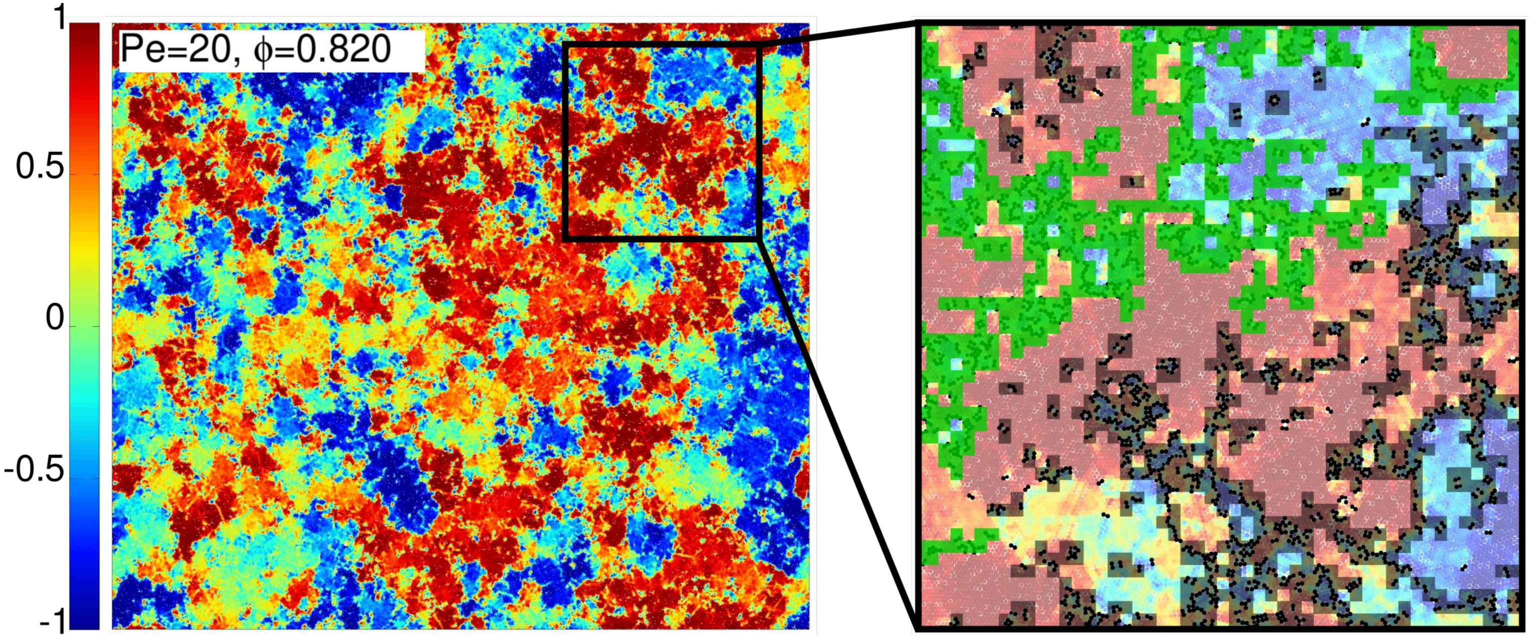

2d active disks: conclusions

- Regardless of the self-propulsion strength, melting proceeds like a two-step KTHN melting.
- First-order to continuous crossover for liquid-hexatic transition with increasing activity.
- For high-enough activity, the dense phase in MIPS is hexatic or even solid.
- General percolation behavior at the hexatic-liquid transition.

Self-propelled dumbbells

In nature, motile objects are most likely to have elongated shape.
We studied a simple model of elongated self-propelled particles, which maintain hexatic order and show non trivial aggregation behaviors.

Interacting self-propelled dumbbells

$$m\ddot{\mathbf{r}}_i = -\gamma\dot{\mathbf{r}}_i - \frac{\partial U_{FENE}}{\partial r_{i,i+1}}\,\hat{\mathbf{r}}_{i,i+1} - \sum_{j\neq i}^{2N}\frac{\partial U}{\partial r_{ij}}\,\hat{\mathbf{r}}_{ij} + F_{\text{act}}\hat{\mathbf{n}}_i + \sqrt{2D_0}\,\eta_i\ ,$$

$$m\ddot{\mathbf{r}}_{i+1} = -\gamma\dot{\mathbf{r}}_{i+1} + \frac{\partial U_{FENE}}{\partial r_{i,i+1}}\,\hat{\mathbf{r}}_{i,i+1} - \sum_{j\neq i+1}^{2N}\frac{\partial U}{\partial r_{i+1,j}}\,\hat{\mathbf{r}}_{i+1,j} + F_{\text{act}}\hat{\mathbf{n}}_{i+1} + \sqrt{2D_0}\,\eta_{i+1}$$

- $U(r) = \begin{cases} U_{\text{Mie}}(r) - U_{\text{Mie}}(r_{min}) & \text{if } r < r_{min} \\ 0 \quad \text{if } r \geqslant r_{min} \end{cases}$
- $\mathbf{F}_{FENE} = -\dfrac{k(\mathbf{r}_i - \mathbf{r}_j)}{1 - r_{ij}^2/r_0^2}$
- $\langle \eta_i(t)\rangle = 0\ , \quad \langle \eta_i^\alpha(t_1)\cdot\eta_j^\beta(t_2)\rangle = \delta_{ij}\delta^{\alpha\beta}\delta(t_1 - t_2)$

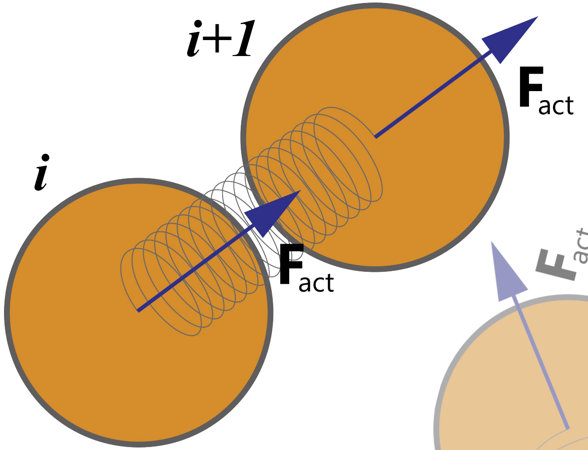

Interacting self-propelled dumbbells

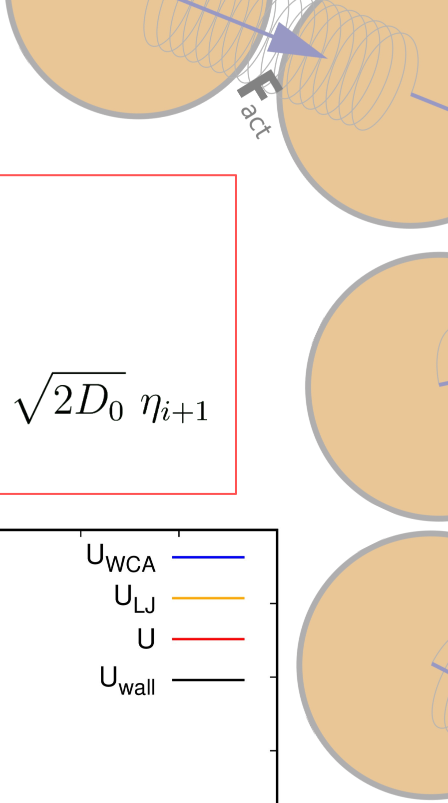

$$m\ddot{\mathbf{r}}_i = -\gamma\dot{\mathbf{r}}_i - \frac{\partial U_{FENE}}{\partial r_{i,i+1}}\,\hat{\mathbf{r}}_{i,i+1} - \sum_{j\neq i}^{2N}\frac{\partial U}{\partial r_{ij}}\,\hat{\mathbf{r}}_{ij} + F_{\mathrm{act}}\hat{\mathbf{n}}_i + \sqrt{2D_0}\,\eta_i\ ,$$

$$m\ddot{\mathbf{r}}_{i+1} = -\gamma\dot{\mathbf{r}}_{i+1} + \frac{\partial U_{FENE}}{\partial r_{i,i+1}}\,\hat{\mathbf{r}}_{i,i+1} - \sum_{j\neq i+1}^{2N}\frac{\partial U}{\partial r_{i+1,j}}\,\hat{\mathbf{r}}_{i+1,j} + F_{\mathrm{act}}\hat{\mathbf{n}}_{i+1} + \sqrt{2D_0}\,\eta_{i+1}$$

- $$U(r) = \begin{cases} U_{\mathrm{Mie}}(r) - U_{\mathrm{Mie}}(r_{min}) & \text{if } r < r_{min} \\ 0 \quad \text{if } r \geqslant r_{min} \end{cases}$$

$$U_{\mathrm{Mie}}(r) = 4\varepsilon\left[\left(\frac{\sigma}{r}\right)^{64} - \left(\frac{\sigma}{r}\right)^{32}\right]$$

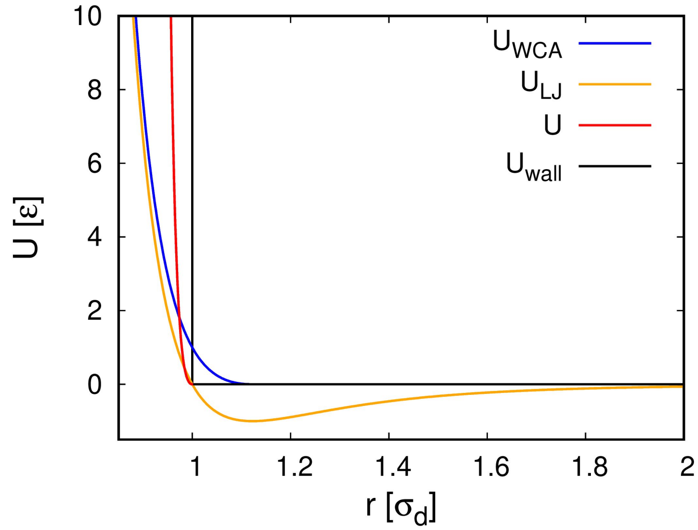

Phase diagram for active dumbbells

- Liq-hex coexistence at any Pe
- Continuously connected coexistence region

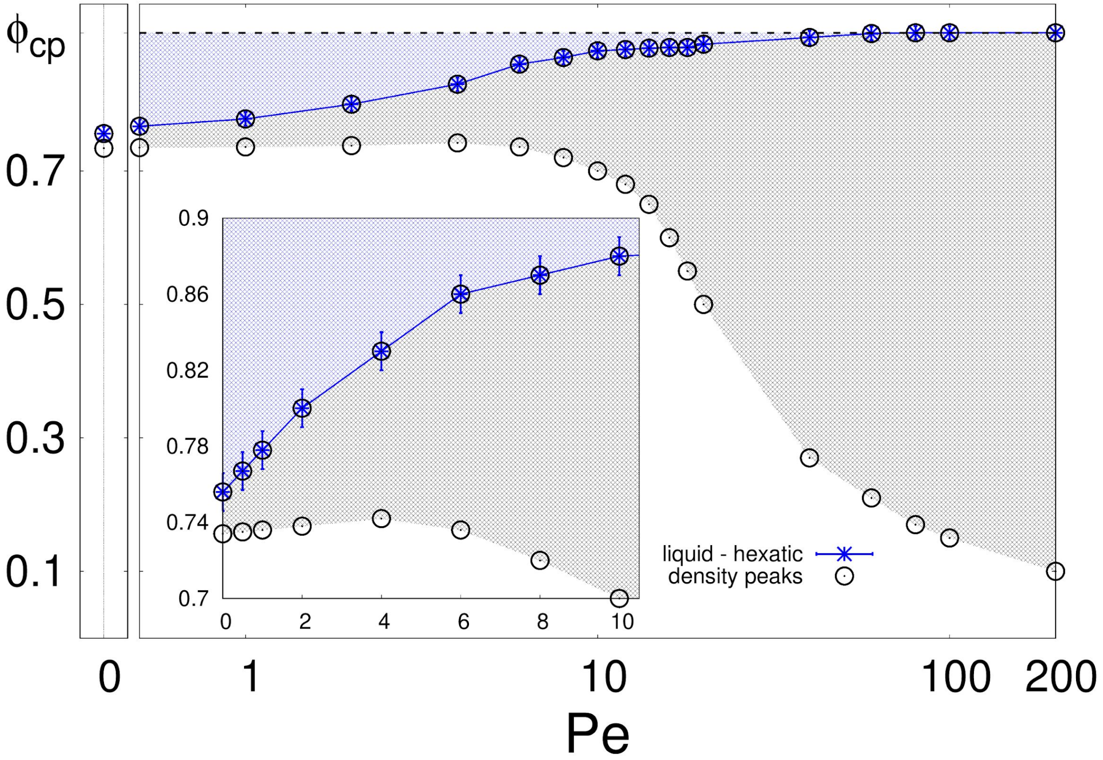

Cugliandolo L.F., Digregorio P., Gonnella G., Suma A., Phys. Rev. Lett., 119 268002 (2017)

Non trivial pattern formation and sustained cluster rotation

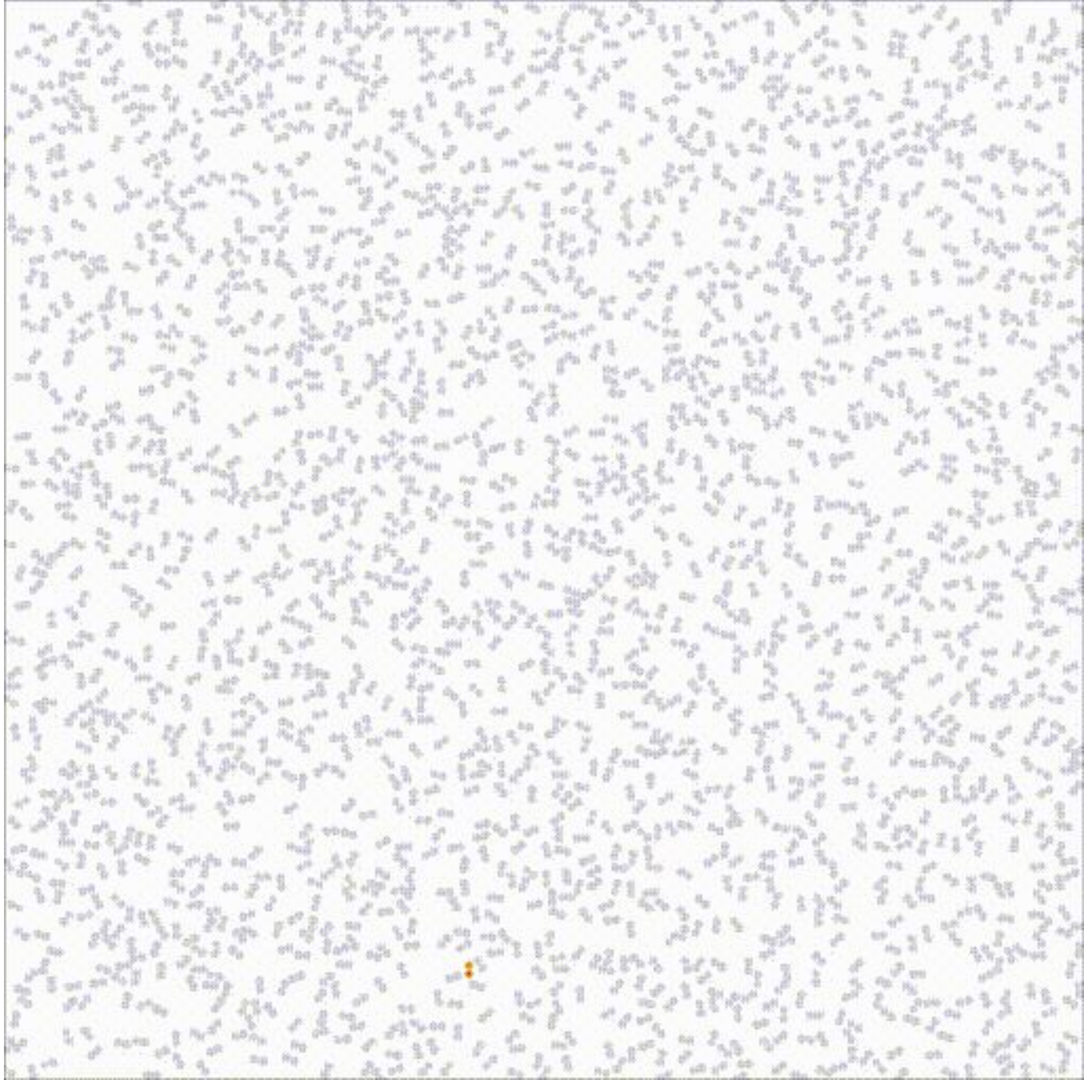

Non trivial pattern formation and sustained cluster rotation

Velocity (vortex)

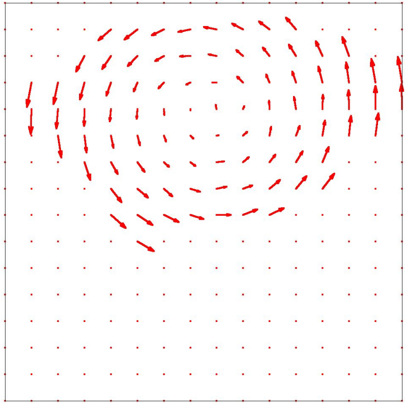

Polarization (spiral)

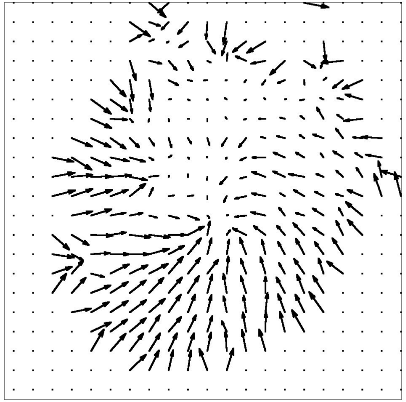

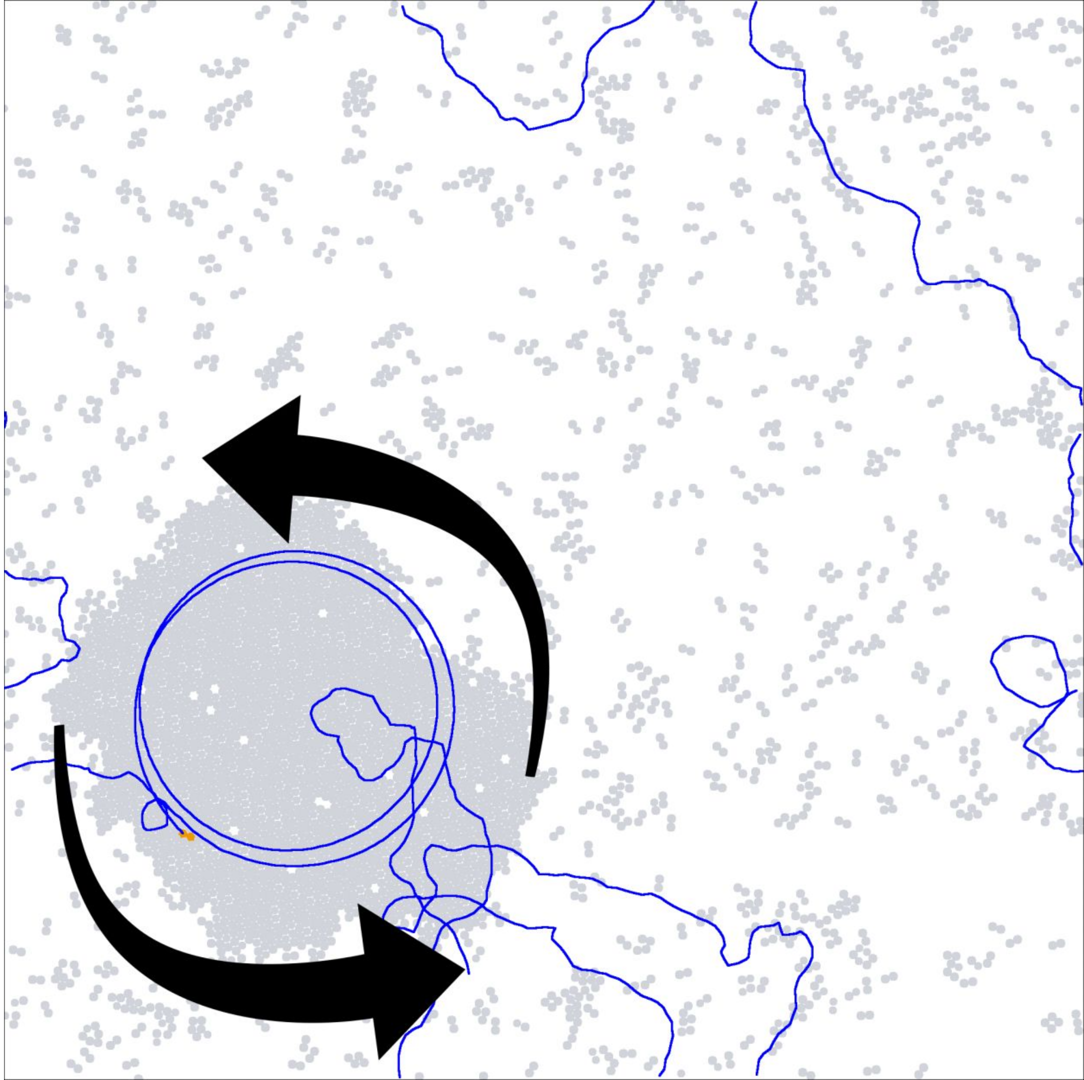

Outlooks

- Phase diagram, MIPS and hexatic order of elongated objects which interpolate between disks and dimers. We expect that, starting from the dumbbells, if we let the two beads to overlap of a given fixed extent, the system will lose the hexatic order even at very high global density.

- Analysis of the growing dynamics and the stationary properties of hexatic domains in quenching process into the coexistence region.

Publications and proceedings

- **PD, D. Levis, L.F. Cugliandolo, G. Gonnella, I. Pagonabarraga**. arXiv:1911.06366 (2019).
- **G. Negro, L.N. Carenza, PD, G. Gonnella, A. Lamura**, AIP Conference Proceedings, 2071, 1 (2019).
- **PD, D. Levis, A. Suma, L. F. Cugliandolo, G. Gonnella, I. Pagonabarraga**, Journal of Physics: Conference Series 1163 (2019).
- **I. Petrelli, PD, L.F. Cugliandolo, G. Gonnella, A. Suma**, Eur. Phys. J. E, 41(10):128, (2018).
- **PD, D. Levis, A. Suma, L.F. Cugliandolo, G. Gonnella, I. Pagonabarraga**, Phys. Rev. Lett., 121, (2018).
- **G. Negro, L.N. Carenza, PD, G. Gonnella, A. Lamura**, Physica A: Statistical Mechanics and its Applications, 503, (2018).
- **L. F. Cugliandolo, PD, G. Gonnella, A. Suma**, Phys. Rev. Lett., 119:119, (2017).

Thank you!